doi.org/10.36721/PJPS.2023.36.1.REG.171-180.1

Intestinal transport mechanism of HA-LOR microspheres with different molecular weights in the MDCK cell model

Wantong Zhao[1], Lin Ma[1], Changxiu Lin[3], Jingshu Piao[1] and Mingguan Piao[1,2]*

[1]College of Pharmacy, Yanbian University, Yanji, P.R. China
[2]Key Laboratory of Natural Medicines of the Changbai Mountain, Ministry of Education, Yanbian University, Yanji, P.R. China
[3]Central laboratory of Affiliated Hospital of Yanbian University, Yanji, P.R. China

Abstract: In this study, LOR microspheres with different molecular weights of hyaluronic acid (HA) were prepared by spray drying method using the second-generation antihistamine loratadine (LOR) as a model drug. A small intestinal transmembrane transport model was used to study the effect of HA molecular weight on small intestinal transmembrane transport and to explore the mechanism of HA molecular weight on intestinal absorption. The transmembrane transport of HA-LOR microspheres of different molecular weights was investigated by adding several inhibitors related to drug transmembrane transport and cellular function in the MDCK cell model. The results showed that low, medium and high molecular weight HA in HA-LOR microspheres had no effect on P-gp efflux and macrocytidine and had no effect on the transmembrane of LOR microspheres; medium molecular weight HA could affect Ca^{2+} channel and has an effect on the transmembrane transport of LOR microspheres; high molecular weight HA can affect clathrin-mediated endocytosis, lipid microcapsule-mediated endocytosis and endosomes, indicating that high molecular weight HA-LOR microspheres are effective in the intestinal tract. The uptake of LOR can be facilitated by the action of uptake enhancers, the action of Ca^{2+} channels and the uptake of ATP to LOR.

Keywords: Hyaluronic acid, loratadine, microsphere, intestinal transport mechanism, transport inhibitors.

INTRODUCTION

Loratadine (LOR), a second-generation antihistamine, is a highly effective antiallergic drug widely used to treat allergies such as runny nose, sneezing, skin rashes and hives (Nakamura *et al.*, 2019, Iesce *et al.*, 2019). Compared with other antihistamines, the drug has few side effects, including tiredness, drowsiness, dry mouth and headache. Although side effects are few, poor bioavailability due to low solubility is a significant disadvantage. The solubility in water is less than 1mg/mL at 25°C and the logP value is 2.83. Improving the solubility of loratadine is a major research topic.

Hyaluronic acid (HA) is a linear macromolecular mucopolysaccharide that consists of two sugar units alternately connected by glucuronic acid and N-acetylglucosamine with molecular weights ranging from 5000 to 2×10^7 Da. In its natural state, HA is a large molecule that is fragmented to lower molecular weights forms in tumors during inflammatory cell infiltration (Liu *et al*., 2019, Sun *et al*., 2019., Hamilton M *et al.*, 2021) High and low molecular weight HA participates in many biological functions (Zhang *et al*., 2017, Palumbo *et al*., 2017, Cañibano-Hernández *et al*., 2019). The penetration of HA is related to its molecular weight and appropriate molecular weights HA can be selected according to its specific purpose (Marinho A *et al*., 2021).

Microspheres are drug carriers that can be used to achieve sustained release by regulating and controlling the release rate of drugs. They can also protect drugs from degradation by enzymes in the body which give them favorable characteristics including reducing the dosing frequency, reducing toxicity and improving efficacy (Kim *et al*., 2021). In this study, LOR was used as a model drug and different molecular weights of HA and PEG6000 were used as carrier materials to prepare LOR microspheres to improve the solubility and dissolution rate of insoluble drugs in water.

Oral administration is one of the most commonly used routes of drug administration and provides very good patient compliance. Oral drugs are mainly absorbed by passive diffusion that is mainly restricted by the plasma membrane of the small intestinal epithelial cells or tight junctions between epithelial cells (Jinhua., 2019, Suzuki., 2020, Subramanian *et al*., 2022). Small molecule drugs can also be actively transported through epithelial cells, whilst large molecules are more likely to be transported via pinocytosis (Jøraholmen *et al*., 2017). The mechanisms involved in the transmembrane transport of drugs are diverse. However, most drugs pass through epithelial cells. The oral micro particle delivery system ensures that the formulation reaches the gastrointestinal tract to effectively release the drug and it also needs to be able to cross the gastrointestinal barrier unique to oral absorption. The transmembrane transport of cells is closely related to the endocytosis of the preparation. Current research has found that the endocytosis mechanisms of different cells used in micro particle drug delivery systems are mainly divided into phagocytosis and pinocytosis. Therefore, detailed analysis of endocytosis characteristics is very necessary.

*Corresponding author: e-mail: mgpiao@ybu.edu.cn

MDCK (Madin-Daby canine kidney cells) are often used to study the mechanisms of drug absorption and transport in the small intestine (Ling *et al.,* 2017, Khatri and Shao, 2018). In this study, MDCK cells were used to establish a transwell transmembrane transport model to evaluate the transport of HA-LOR microspheres. Use different endocytosis inhibitors and cell signaling transduction-related inhibitors or agonists to investigate the mechanism of transmembrane transport and the absorption of HA LOR microspheres of different molecular weights in the small intestine. These drugs included amiloride hydrochloride (Yasen *et al*., 2018), chlorpromazine hydrochloride (Xia *et al*., 2018, Yasen *et al*., 2018), methyl β-cyclodextrin (M-β-CD) (Xia *et al*., 2018), monensin, sodium deoxycholate, iodoacetamide (2018, Ma *et al*., 2018), verapamil and EDTA (2018, Ma *et al*., 2018).

In summary, this study use spray drying to prepare LOR microspheres with different molecular weights and conduct *in vitro* studies. Using the MDCK cell transwell model, different endocytosis inhibitors and cell signal transduction-related inhibitors or agonists use to study the effect of the molecular weight of HA on the transmembrane transport of LOR in the small intestine mucosa.

MATERIALS AND METHODS

Materials

LOR was purchased from the Jinan Dexinjia Biotechnology Co., Ltd (Jinan China). PEG 6000 and ethanol were purchased from the Tianjin Komi Chemical Reagent Co., Ltd (Tianjin China). HA was purchased from the Zhenjiang Dongyuan Biotechnology Co., Ltd (Zhenjiang China). MDCK cells [NBL-2] were purchased from the Wuhan Punose Life Technology Co, Ltd (Wuhan China). MTT (Thiazolyl Blue Tetrazolium Bromide), PBS and HANKS were purchased from Solarbio. Trypsin-EDTA, DMEM (Dulbecco's Modified Eagle Medium) and FBS (Fetal Bovine Serum) were purchased from BI (Biological Industries). Transwell was purchased from Corning (12mm Diameter inserts, Polycarbonate Membrane). Verapamil, chlorpromazine hydrochloride, methyl-β-cyclodextrin, iodoacetamide, monensin and EDTA were purchased from the Shanghai Aladdin Biochemical Technology Co, Ltd (Shanghai, China). Amiloride and sodium deoxycholate were purchased from MedChemExpress.

Preparation of HA-LOR microspheres with different molecular weights

Precise amounts of LOR were weighed and dissolved in ethanol. The required amounts of HA and PEG6000 were dissolved in specific volumes of water. The two solutions were mixed evenly (1:2, v/v) and a mixed solution obtained using a spray drying method to generate the HA-LOR microspheres. The preparation parameters are as follows; an inlet air temperature of 135^{O}C, an outlet air temperature of 98^{O}C, an atomization pressure of 10×10 Kpa, an inlet air volume 0.50 m³·min and a flow rate 160mL/h.

The prescription of HA-LOR microspheres with different molecular weights was performed using spray drying technology. The prescription s is summarized in table 1.

Evaluation of HA-LOR microspheres with different molecular weights

Surface morphology and particle sizes

The morphology of HA-LOR microspheres with different molecular weight was determined by scanning electron microscopy (SEM). Take an appropriate amount of HA-LOR microspheres from each prescription in table 1 and add a certain amount of distilled water to make a suspension solution. 3 mL of suspension sample was used and the particle sizes determined using a laser particle size analyzer. The measurement parameters were set as follows; a temperature of 25°C, an equilibrium time of 3 mins and a He-Ne laser source with a wavelength of 633 nm.

Determination of solubility

LOR and the microspheres of various prescriptions were placed in centrifuge tubes with distilled water and placed in a constant temperature shaker at 25°C for 3 days to make them supersaturated. Samples were centrifuged for 5 minutes at 1300 rpm and the supernatant filtered through a 0.45 μm microporous membrane. The filtrate was analyzed by HPLC and the solubility of LOR in the microspheres and LOR in water calculated.

Determination of drug loading and drug loading rate

5mg of HA-LOR microspheres were added to 5 mL of ethanol (50%) and shaken for 3 days. After passing through a 0.45μm microporous membrane, the filtrate was analyzed by HPLC. LOR drug loading and the drug loading rates were calculated.

Formulas for calculating drug loading and drug loading rate of microspheres:

Drug loading (%) = (weight of drug contained in microspheres/ total weight of microspheres) ×100%

Drug loading rate (%) = (actual dosage in microspheres/ theoretical dosage in microspheres) ×100%

Determination of cumulative release in vitro

According to the release determination method in Appendix 2 of the Chinese Pharmacopoeia (2015 edition), the speed is set at 100 rpm, the temperature is set at 37 ± 0.5°C, the dissolution medium is distilled water and the volume is 900mL. The dosage of HA-LOR microspheres is equivalent to 600μg of LOR. 5 mL of filtrate is sampled at 10, 20, 30, 60, 90, 20, 180, 240, 360, 540 and 720 min, after passing through a 0.45 μm micro porous membrane, the filtrate was analyzed by HPLC. calculated the drug concentration and the drug dissolution percentage.

The cumulative release percentage Q (%) of the drug in microspheres was calculated according to the following formula.

$$Q = \frac{\sum_{i=1}^{n-1} C_1 V_1 + C_n V}{M} \times 100\%$$

In the formula, C_1 is the mass concentration of the drug measured at the first sampling point, C_n is the mass concentration of the drug measured at the nth ($n \leq n-1$) sampling point, V_1 is the volume of the dissolution release medium (900mL), V is the sampling volume (5mL in this experiment) and M is the dosage quality.

MTT assay

MTT assay for cytotoxicity of LOR and HA-LOR microspheres

The toxicity of LOR and HA-LOR microspheres in MDCK cells was determined after 4 h. 50 mg of LOR was weighed, dissolved in HANKS solution and diluted into suspension at concentrations of 0.01, 0.1, 1, 5 and 10mg/mL. MDCK cells were inoculated into 96-well plates at a density of 2×10^5 per well. 0.2mL of cell suspension was added into each well. After incubation at 37^OC in a 5%CO_2 incubator, the medium was removed and the diluted series of solutions were added to each well. No drug was added to the blank control well. After incubation for 4h, 20μL of 5g/L MTT was added to each well. After a further 4 hours incubation, the supernatant was removed and 150μL of DMSO added to each well. Plates were then shaken for 10 min at low speed to allow the MTT crystals to completely dissolve. The absorbance of each well was measured at 490 nm.

The survival rate (IC) was expressed as IC%= mean A of experimental group/mean A of control well ×100%.

MTT assay for cytotoxicity of different inhibitors

The cytotoxicity of different transport inhibitors (amiloride hydrochloride, chlorpromazine hydrochloride, methyl-beta-cyclodextrin, monensin, sodium deoxycholate, iodoacetamide, verapamil and EDTA) was determined in MDCK cells after 4 h. 1.2 mg of amiloride hydrochloride was dissolved in HANKS solution with mixing for 5 min and diluted to concentrations of 1, 2.5 and 5 μmol/L. 1.78 mg of chlorpromazine hydrochloride was weighed and dissolved in HANKS solution with mixing for 5 min and diluted to concentrations of 50, 100 and 200 μmol/L. 32.58 mg of M-*β*-CD was dissolved in HANKS solution with mixing for 5 min and diluted to concentrations of 1, 2.5 and 5 mmol/L solution. 1.3 mg of monensin was dissolved in HANKS solution with mixing for 5 min and diluted to concentrations of 8, 16 and 32.5 μg/L. 0.66 mg of sodium deoxycholate was dissolved in HANKS solution with mixing for 5 min and diluted to concentrations of 50, 100 and 200 μmol/L. 0.37 mg of iodoacetamide was dissolved in HANKS solution with mixing for 5 min and diluted to concentrations of 10, 25, 100 μmol/L. 1.23 mg of Verapamil was dissolved in HANKS solution with mixing for 5 min and diluted to concentrations of 25, 50 and 100μmol/L solution. 6 mL of EDTA was dissolved in HANKS solution with mixing for 5 min and diluted to concentrations of 1, 2.5 and 5mmol/L solution. The operation and measurement methods are the same as described in 2.4.1.

Establishment of the MDCK cell transmembrane transport model

MDCK cell culture

MDCK cells were cultured in DMEM medium containing 10% FBS. Cell media was aspirated and the concentration of cells adjusted to 2×10^5 cells/mL and 0.5mL added to the upper. 1.5 mL of DMEM culture medium containing 10% FBS was added to the lower well the transwell and cultured at 37°C and 5% CO_2. The culture liquid was changed the next day after the cell laying and then every other day. The same amount of complete DMEM (upper 0.5 mL, lower 1.5 mL) was used to replace the media. When the media was changed, the lower layer was sucked first and then the upper layer was sucked. The upper layer was replaced with 0.5 mL and the lower layer was replaced with 1.5mL.

The transmembrane resistance of MDCK cells at different times was measured using a Millicell® ERS-2 system. When the transmembrane resistance reached more than 250 $\Omega \cdot cm^2$, the next transmembrane transport experiment was carried out.

Transmembrane transport of HA-LOR microspheres with different molecular weights in the MDCK cell model

The transmembrane transport of HA-LOR microspheres with different molecular weight based on MDCK cell model was studied. The Transwell was washed with HANKS solution and the Transwell was added with the same amount of HANKS solution at 37^OC to stabilize the cell. After 30 min, HANKS solution was sucked out.

According to the experimental group, 0.1, 0.3 and 1mg/mL LOR and high molecular weight HA-LOR microspheres were added to study the transport experiment of HA-LOR microspheres with the same molecular weight and different concentrations.

0.3mg/mL LOR and HA-LOR microspheres with different molecular weights, to study the transport experiment of HA-LOR microspheres with different molecular weights and the same concentration. And incubate in a cell culture incubator at 37°C.

At 0.5, 1, 1.5, 2 and 4 h, 1 mL of liquid was taken from the lower layer (after the same amount of HANKS was added) and determined by HPLC.

The cumulative permeation amount Q is calculated according to the formula and then plotted by the ratio of the cumulative permeation amount Q to the time T.

$$Q = \frac{(C_n \times V + \sum_{n=1}^{i=n-1}[C_i V_i)]}{A}$$

In the formula, C_n is the mass concentration of the drug measured at the n-th sampling point, C_i is the mass concentration of the drug measured at the i-th (i≤n-1) sampling point, V is the volume of the diffusion cell (1.5mL) and V_i is Sampling volume (1 mL in this test), A is the effective area (1.12 cm^2 in this test).

Transport mechanism of HA-LOR microspheres with different molecular weight in the MDCK cell model

The transport mechanism of HA-LOR microspheres with different molecular weights was investigated in the MDCK cell model. HANKS solution was used to wash the transwell as previously described. The same amount of HANKS solution was added to each transwell and the cells incubated at 37°C for 30 min. The HANKS solution was removed and grouped according to the experimental group, 0.3 mg/mL HA-LOR microspheres with different molecular weights are used as the control group, 0.3 mg/mL HA-LOR microspheres with different molecular weights and amiloride hydrochloride are used as the experimental group. (taking amiloride hydrochloride as an example). 0.5 mL of amiloride hydrochloride inhibitor solution was first added to transwell and incubated at 37°C for 30 min and washed with HANKS solution. Different drugs were added and incubated at 37^{O}C. At 0.5, 1, 1.5, 2, 4 h, 1 mL of HANKS solution was removed from the lower layer (after the same amount of HANKS was supplemented) and analyzed by HPLC.

The cumulative permeation amount Q is calculated according to the formula and then plotted by the ratio of the cumulative permeation amount Q to the time T.

$$Q = \frac{(C_n \times V + \sum_{n=1}^{i=n-1}[C_i V_i)]}{A}$$

STATISTICAL DATA ANALYSIS

The experiments were repeated thrice and all evaluations were performed in triplicate. Multiple groups were analysed employing one-way ANOVA. The statistical software Graphpad Prism5 (GraphPad, Sandiego, CA, USA) was used to process the data and the mean value of the data was expressed as ±SEM. Dunnett's Stest was used for statistical analysis of relevant data by One-way-ANOVA method. $P < 0.05$ in the chart indicated significant and statistically significant data difference. The data were processed by statistical software and the experimental results were obtained.

RESULTS

Preparation and evaluation of HA-LOR microspheres with different molecular weights

Surface morphology

The HA-LOR microspheres were analyzed by scanning electron microscopy (SEM) (fig. 1). The results showed that the microspheres were spherical and the viscosity of the solution increased with increasing molecular weight of HA which resulted in adhesion of HA-LOR microspheres.

Particle sizes

The average particle size was measured by a laser particle size analyzer (fig. 2A) and showed the size of the microspheres increased with an increasing molecular weight of HA.

Determination of solubility

The solubility of LOR and LOR in the microspheres (fig. 2B) were determined. The solubility of LOR is 1.07 ± 0.05 µg/mL and the solubility in prescriptions I, II and III microspheres is 1.43 ± 0.09µg/mL, 2.70 ± 0.20 µg/mL and 15.35 ± 0.43µg/mL. From fig. 2B it can be seen that the solubility of LOR microspheres increased with an increasing molecular weight of HA and the solubility was higher than that of LOR.

Determination of drug loading and drug loading rate

The drug loading and drug loading rates of the microspheres are presented as a bar graph (fig. 2C, fig. 2D). From fig. 2C, it can be seen that the drug loading of the microspheres decreased with an increasing molecular weight of HA (Prescriptions I, II and III drug loadings are 8.76 ± 0.12%, 8.50 ± 0.07%, 8.08 ± 0.38%). There were no significant differences between prescription I, II and III. From fig. 2D, the drug loading rate of the microspheres decreased with increasing molecular weight of HA (Prescription I, II and III drug loading rates are 83.23 ± 0.12%, 80.72 ± 0.07%, 76.72 ± 0.38%).

Determination of cumulative release in vitro

The paddle method was used to determine the cumulative dissolution rate of the microspheres and the raw materials at different times. The results showed that the dissolution rate of LOR *in vitro* was significantly increased after the preparation of HA-LOR microspheres. HA in prescription III was significantly increased compared to the raw materials (fig. 2E). The cumulative release rate of HA-LOR microspheres in prescription III was the highest *in vitro* at 12 h at 83.19±1.82%.

MTT assay for cytotoxicity of LOR and HA-LOR microspheres

The toxicity of LOR and LOR microspheres in MDCK cells was determined after 4h. The absorbance of each well was measured at 490nm using an enzyme labeling instrument. The results showed that LOR and LOR microspheres with concentrations of 0.01, 0.1, 1.0mg/mL were not toxic in MDCK cells after 4h (fig. 3A).

MTT assay for cytotoxicity of different inhibitors

The toxicity of different inhibitors in MDCK cells was determined after 4h. The absorbance of each well was measured at 490nm with an enzyme label. The results presented in fig. 3B show the toxicity of different inhibitors

at different concentrations for 4h (+4h after MTT) in MDCK cells. (1) Verapamil is not toxic at 25μmol/L and toxic at 50 and 100μmol/L. (2) EDTA: 1, 2.5, 5mmol/L, MTT results showed that all three concentrations were toxic, but there was no difference among the three concentrations. After adding MTT, it is found that the crystallization of methylamine in this group is different from that in other groups. The crystallization in this group is a large block, while the crystallization in other groups is fine crystals with uniform distribution. Therefore, the toxicity of this drug may be pseudo toxicity, so it is only for reference. (3) Chlorpromazine hydrochloride is non-toxic at 50μmol/L and toxic at 100 and 200μmol/L (4) M-*β*-CD: 1,2.5mmol/L is non-toxic; 5mmol/L is toxic. (5) Amiloride hydrochloride: 1, 2.5μmol/L is non-toxic, 5μmol/L is toxic. (6) Iodoacetamide is nontoxic at 10 and 25μmol/L and toxic at 100μmol/L. (7) Monensin 8, 16 and 32.5μg/L were non-toxic. (8) Sodium deoxycholate: 50, 100, 200μmol/L are non-toxic.

The final concentration of the inhibitors were as follows; sodium deoxycholate 100μmol/L, EDTA 2.5mmol/L, verapamil 25μmol/L, iodoacetamide 10μmol/L, monensin 32.5μg/L, amiloride 1μmol/L, chlorpromazine hydrochloride 50μmol/L M-*β*-CD 2.5mmol/L.

Transmembrane transport of HA-LOR microspheres in the MDCK cell model

Microsphere transfer experiments of HA LOR with different molecular weights

The cumulative transmittance of all microspheres increased with increasing concentration and time (fig. 4A). The cumulative transmittance of the microspheres was much larger than that of the LOR. The first 2 h of the LOR at low concentration could not be detected because of the low concentration.

Transplantation experiments of HA-LOR microspheres with different molecular weights and concentrations

The cumulative permeability of the HA-LOR microspheres with different molecular weights and same concentration (4.8×10^4 Da HA, 4.6×10^5 Da HA, 1.05×10^6 Da HA) increased with an increasing molecular weight of HA. LOR was detected only at 4h due to its low concentration (fig. 4B).

Investigated the mechanisms of HA-LOR transmembrane transport using specific inhibitors directed against different transporters

Effect of endocytosis mechanism of different molecular weight HA-LOR microspheres

Effect of micropinocytosis

The addition of amiloride hydrochloride (an inhibitor of micropinocytosis) had no significant difference in the cumulative permeability of the microspheres and will not affect the endocytosis (fig. 5A).

Effect of clathrin-mediated endocytosis

Chlorpromazine hydrochloride (clathrin-mediated endocytosis inhibitor) had no significant differences were observed in the cumulative permeation of low molecular and medium molecular weight HA-LOR microspheres. High molecular weight HA showed a difference at 4 h indicating that it can affect the absorption of LOR by clathrin-mediated endocytosis in the later stages (fig. 5B).

Effects of lipid microcapsule-mediated endocytosis

M-β-CD (lipid microcapsule-mediated endocytosis inhibitor) had no significant differences were observed in the cumulative permeation of low molecular and medium molecular weight HA-LOR microspheres. High molecular weight HA showed a difference at 4 h indicating that it can affect the absorption of LOR by lipid microcapsule-mediated endocytosis in the later stages (fig. 5C).

Effect of endosome function

Monensin (endosomal function inhibitor) had no significant differences were observed in the cumulative permeation of low molecular and medium molecular weight HA-LOR microspheres. High molecular weight HA showed a difference at 4 h indicating that it can affect the absorption of LOR by endosome in the later stages (fig. 5D).

Effect of tight junction absorption of different molecular weight HA-LOR microspheres

Effect of absorption enhancer

The addition of sodium deoxycholate (an inhibitor of absorption enhancer) had no significant differences were observed in the cumulative permeation of low molecular and medium molecular weight HA-LOR microspheres. High molecular weight HA showed a difference at 4 h indicating that it can affect the absorption of LOR by tight junction absorption in the later stages. (fig. 6A).

Effect of Ca^{2+} channel

The addition of EDTA (an inhibitor of Ca^{2+} channel) had no significant differences were observed in the cumulative permeation of low molecular weight HA-LOR microspheres. Medium molecular and high molecular weight HA all showed differences at 4 h indicating that it can affect the absorption of LOR by Ca^{2+} channels in the later stages. (fig. 6B).

Effect of ATP of different molecular weight HA-LOR microspheres

The addition of iodoacetamide (an inhibitor of ATP) had no significant differences were observed in the cumulative permeation of low molecular and medium molecular weight HA-LOR microspheres. High molecular weight HA showed a difference at 4 h indicating that it can affect the absorption of LOR by ATP in the later stages (fig. 7).

Effects of P-gp of different molecular weight HA-LOR microspheres

The addition of verapamil (an inhibitor of p-gp) had no significant difference in the cumulative permeability of the microspheres and will not affect the P-gp (fig. 8).

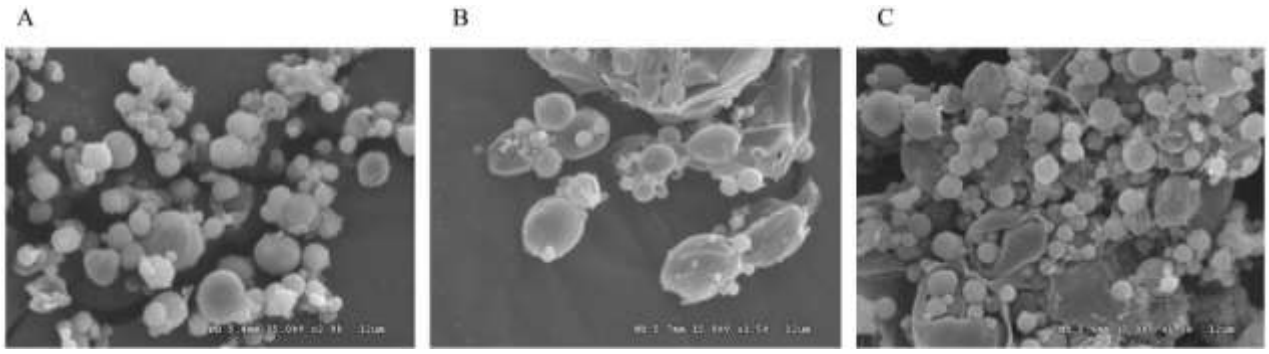

Fig. 1: SEM image of prescription: (A) Prescription I microsphere. (B) Prescription II microsphere. (C) Prescription III microsphere.

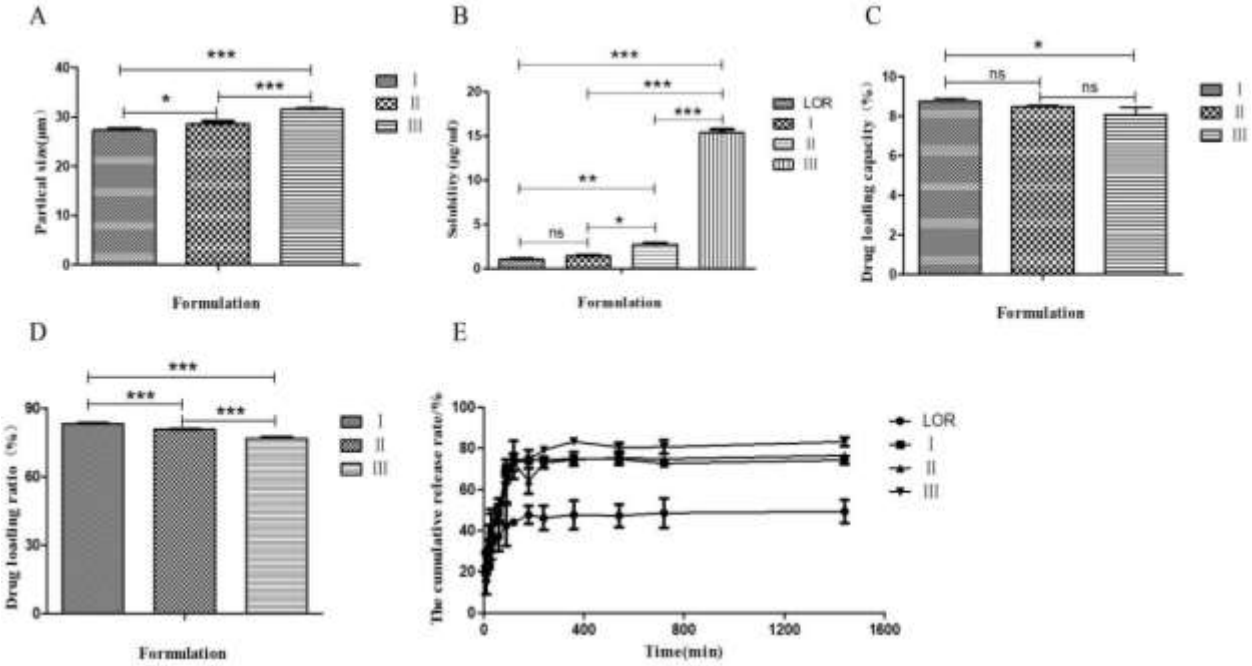

Fig. 2: (A) Bar graph of average particle size measurement results of each prescription microsphere (n=3, *: $p < 0.05$, ***: $p < 0.001$). (B) Solubility of LOR and LOR in microspheres (n=3, *: $p < 0.05$, **: $p < 0.01$, ***: $p < 0.001$). (C) Bar graph of drug loading measurement results of each prescription microsphere (n=3, *: $p < 0.05$). (D) Bar graph of drug loading rate measurement results of each prescription microsphere (n =3, ***: $p < 0.001$). (E) *In vitro* cumulative release of each prescription microsphere and LOR bulk drug (n=3).

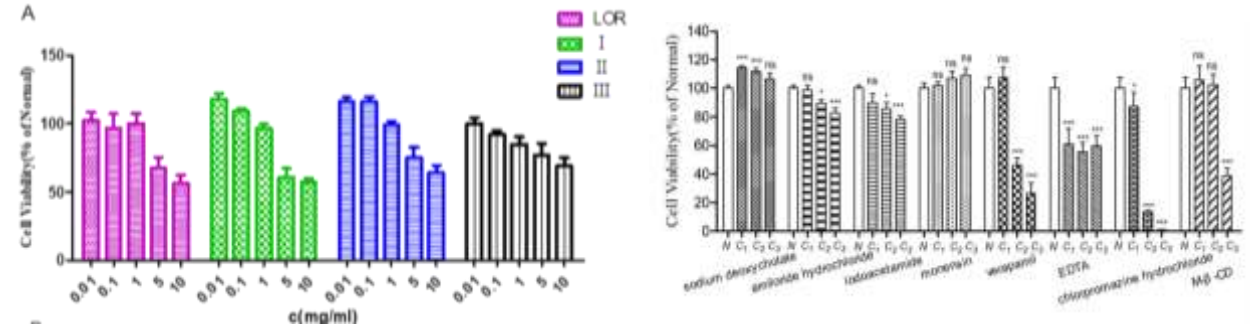

Fig. 3: (A) Totoxicity of LOR and HA-LOR microspheres (n=6). (B)Toxicity of different inhibitors in MDCK cells for 4h (N is the blank group, C_1 is the high concentration group, C_2 is the middle concentration group, C_3 is the low concentration group)(n=3, *: $p < 0.05$, **: $p < 0.01$, ***: $p < 0.001$).

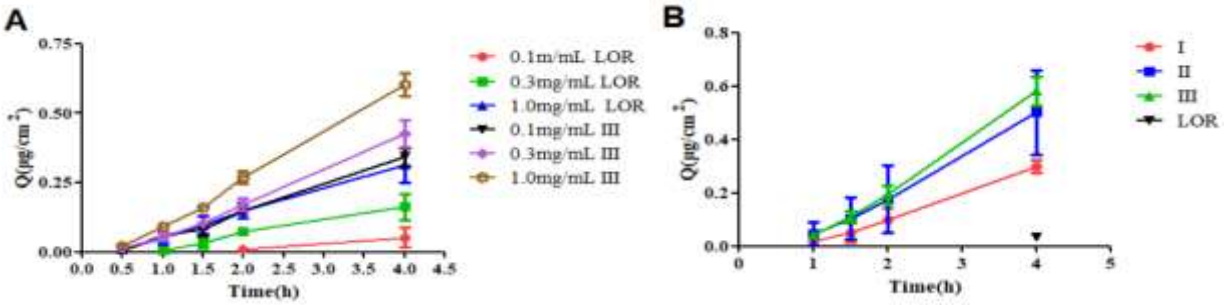

Fig. 4: (A) Cumulative permeability of HA-LOR microspheres with the same molecular weight and different concentrations (n=3). (B) Cumulative permeability of HA-LOR microspheres with different molecular weight and same concentration (n=3).

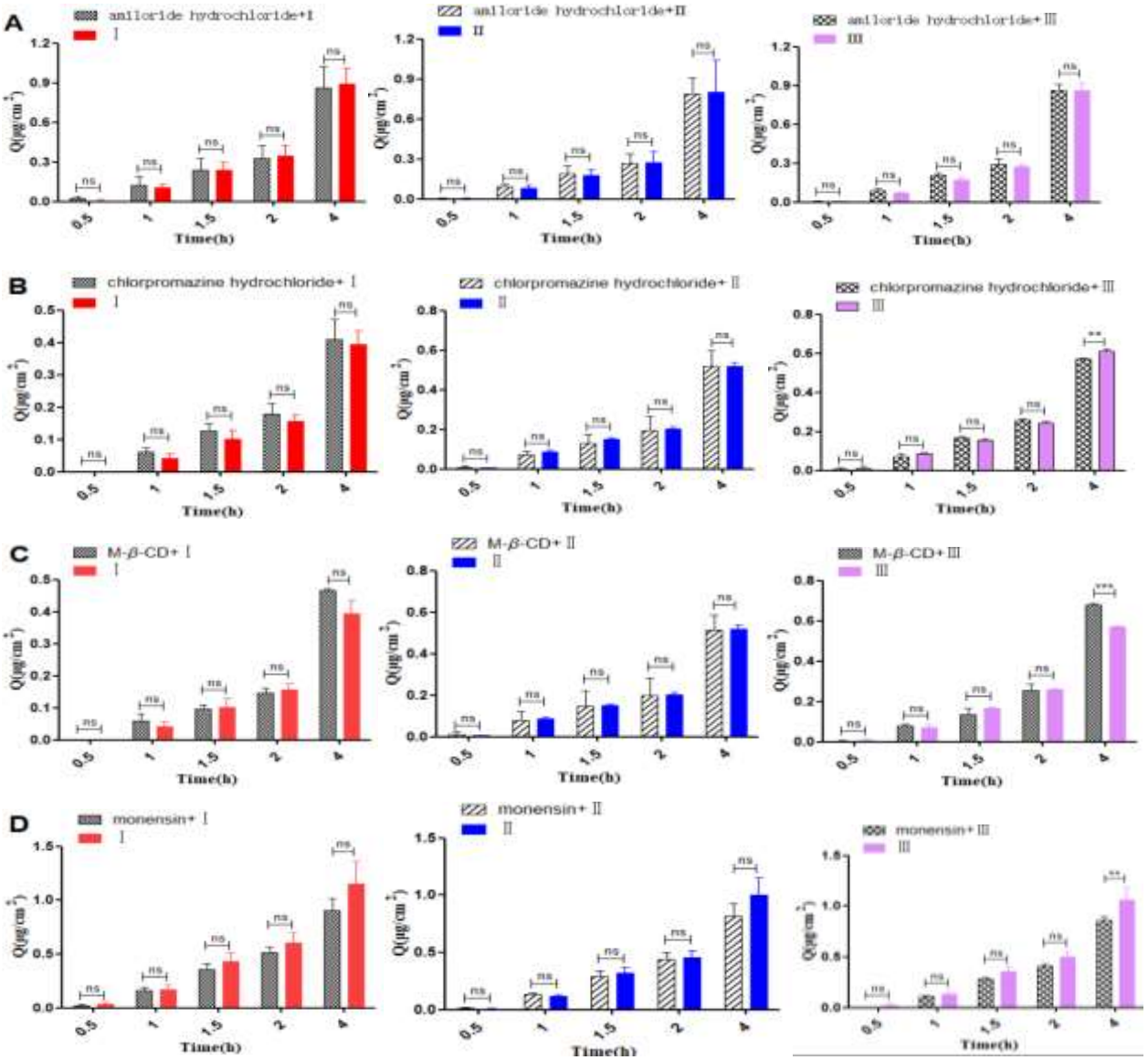

Fig. 5: Effect of endocytosis mechanism on HA-LOR microspheres with different molecular weights: (A) Effect of micropinocytosis. (B) Effect of clathrin-mediated endocytosis. (C) Effects of lipid microcapsule-mediated endocytosis. (D) Effect of endosome function. (n=3, **: $p < 0.01$, ***: $p < 0.001$).

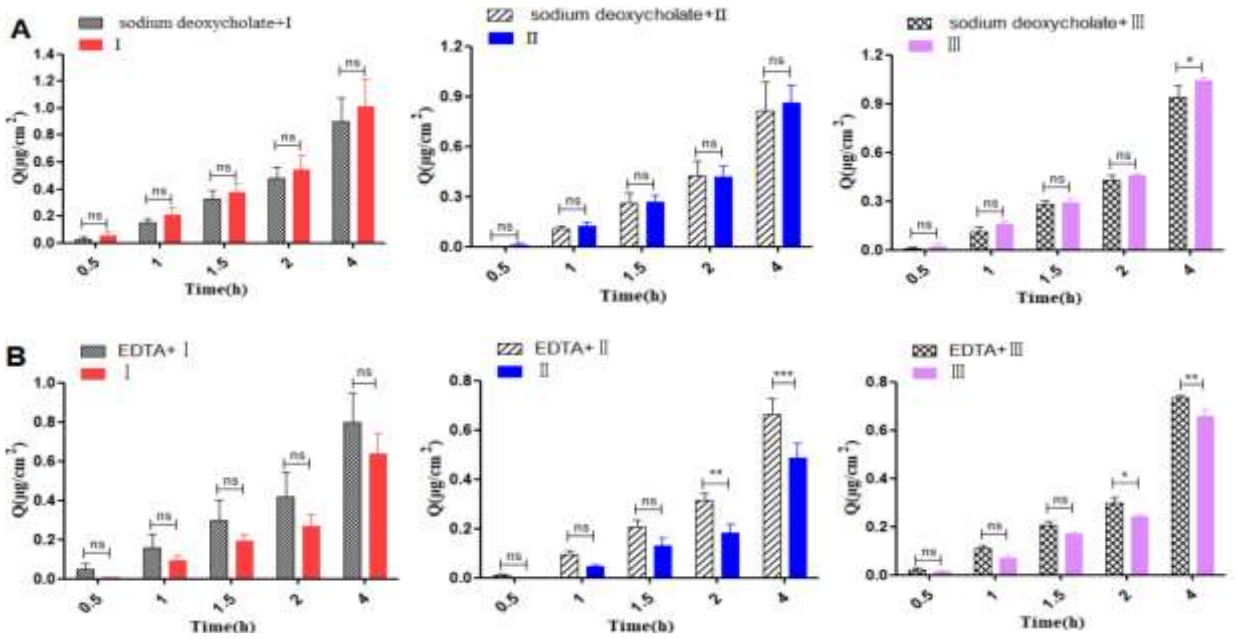

Fig. 6: Effect of tight junction absorption on HA-LOR microspheres with different molecular weights:(A) Effect of absorption enhancer. (B) Effect of Ca^{2+} channel. (n=3, *: $p < 0.05$, **: $p < 0.01$, ***: $p < 0.001$).

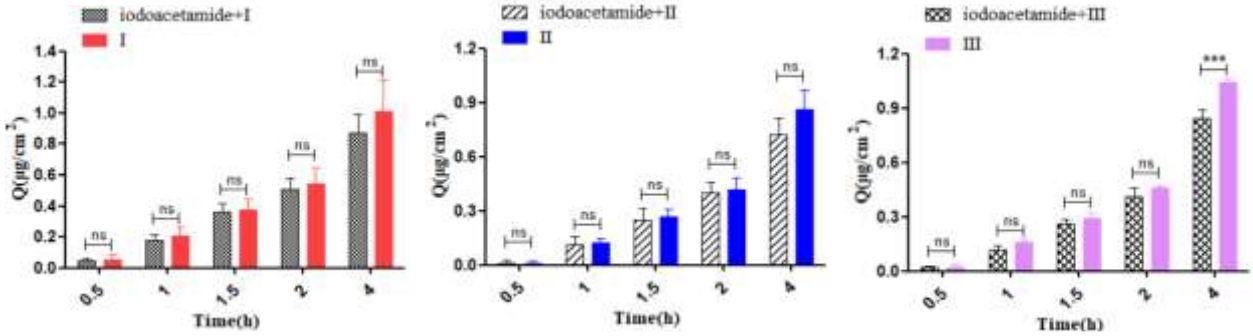

Fig. 7: Effect of ATP of different molecular weight HA-LOR microspheres. (n=3, ***: $p < 0.001$).

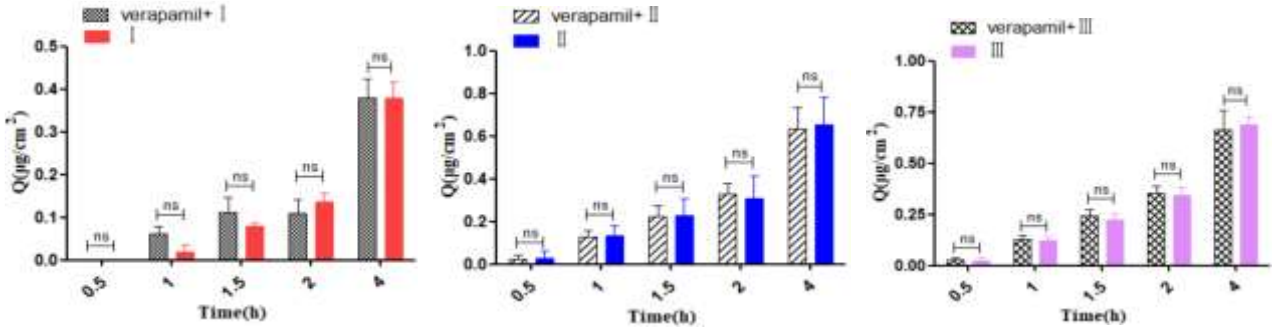

Fig. 8: Effects of P-gp of different molecular weight HA-LOR microspheres. (n=3).

Table 1: Composition of different molecular weight HA-LOR microspheres.

Prescription (g)	I	II	III
16	4.8×10^4 Da HA	4.6×10^5 Da HA	1.05×10^6 Da HA
1	PEG6000	PEG6000	PEG6000
2	LOR	LOR	LOR

DISCUSSIONS

Transmembrane transport mechanism of HA-LOR microspheres with different molecular weights in the small intestine.

There was no significant difference in the cumulative permeability of HA-LOR microspheres with or without the addition of micropinocytosis inhibitor amiloride hydrochloride and P-gp inhibitor verapamil, indicating that micropinocytosis and efflux transporter P-gp did not affect the absorption of HA-LOR microspheres in the intestine.

Transmembrane transport mechanism of low molecular weight HA-LOR microspheres

There was no significant difference in the cumulative permeability of low molecular weight HA-LOR microspheres, indicating that clathrin-mediated endocytosis, lipid microcapsules-mediated endocytosis, endosome function, cellular bypass transport (absorption enhancer), Ca^{2+} channels, and ATP did not affect the absorption of low molecular weight HA-LOR microspheres.

Transmembrane transport mechanism of medium molecular weight HA-LOR microspheres

There was no significant difference in the cumulative permeability of medium molecular weight HA-LOR microspheres, indicating that clathrin-mediated endocytosis, lipid microcapsules-mediated endocytosis, endosome function, cellular bypass transport (absorption enhancer) and ATP did not affect the absorption of absorption molecular weight HA-LOR microspheres. However, Ca^{2+} channels can affect the absorption of HA-LOR microspheres with medium molecular weight.

Transmembrane transport mechanism of high molecular weight HA-LOR microspheres

The was significantly different in the cumulative permeability of high molecular weight HA-LOR microspheres at 4 h, indicating that high molecular weight HA can affect clathrin-mediated endocytosis, lipid microcapsule-mediated endocytosis, endosome function of LOR, cellular bypass transport (absorption enhancer), Ca^{2+} channels, and ATP absorption of LOR. It further affects the absorption of high molecular weight HA-LOR microspheres in the intestine.

CONCLUSION

In this experiment, LOR microspheres with different molecular weights were prepared using a spray drying method. The HA-LOR microspheres were spherical and the particle size increased with increasing molecular weight of HA and the mechanism of the molecular weight of hyaluronic acid on intestinal absorption was discussed. The solubility and *in vitro* cumulative release of LOR in water was positively correlated with the molecular weight of HA. The solubility of 1.05×10^6 Da HA-LOR microspheres was 15.35 ± 0.43 μg/mL and the cumulative release *in vitro* at 12 h was 83.19 ± 1.82%.

A transwell small intestinal transmembrane transport model was established using MDCK cells to simulate the small intestinal mucosa of the human body. The results showed that different molecular weight HA-LOR microspheres increased the cumulative permeation of LOR on the intestinal mucosa in a concentration-dependent manner.

The transmembrane transport of HA-LOR microspheres was investigated by adding several inhibitors related to drug transmembrane transport and cellular function. The results showed the Ca^{2+} channel (EDTA) affected the transmembrane transport of the medium molecular weight HA. The high molecular weight HA was different at 4 h indicating that high molecular weight HA can affect clathrin-mediated endocytosis, lipid microcapsule-mediated endocytosis and endosomal. The absorption of the high molecular weight HA-LOR microspheres in the intestine can be promoted by the action of an absorption enhancer, the action of the Ca^{2+} channel and the absorption of LOR by ATP.

ACKNOWLEDGEMENT

The work was supported by the Key R&D Project of Jilin Province Science and Technology Development Plan of China (No. 20210204166YY).

REFERENCES

Al-Ali AAA, Steffansen B, Holm R and Nielsen CU (2018). Nonionic surfactants increase digoxin absorption in Caco-2 and MDCKII MDR1 cells: Impact on P-glycoprotein inhibition, barrier function and repeated cellular exposure. *Int J Pharm.*, **551**(1-2): 270-280.

Cañibano-Hernández A, Saenz Del Burgo L, Espona-Noguera A, Orive G, Hernández RM, Ciriza J and Pedraz JL (2019). HA enhances cell survival of encapsulated insulin-producing cells in alginate-based microcapsules. *Int J Pharm.*, **557**: 192-198.

Hamilton M, Harrington S, Dhar P and Stehno-Bittel L (2021). Hyaluronic acid hydrogel microspheres for slow release stem cell delivery. *ACS Biomater Sci Eng.*, **7**(8): 3754-3763.

Iesce MR, Lavorgna M, Russo C, Piscitelli C, Passananti M, Temussi F, DellaGreca M, Cermola F and Isidori M (2019). Ecotoxic effects of loratadine and its metabolic and light-induced derivatives. *Ecotoxicol Environ Saf.*, **170**: 664-672.

Jøraholmen MW, Basnet P, Acharya G and Skalko-Basnet N (2017). PEGylated liposomes for topical vaginal therapy improve delivery of interferon alpha. *Eur J Pharm Biopharm.*, **113**: 132-139.

Jinhua W (2019). Ursolic acid: Pharmacokinetics process *in vitro* and *in vivo*, a mini review. *Arch Pharm (Weinheim)*, **352**(3): e1800222.

Khatri P and Shao J (2018). Impact of digestion on the transport of dextran-loaded self-emulsified nanoemulsion through MDCK epithelial cell monolayer and rat intestines. *Int J Pharm.*, **536**(1): 353-359.

Kim JH, Ryu CH, Chon CH, Kim S, Lee S, Maharjan R, Kim NA and Jeong SH (2021). Three months extended-release microspheres prepared by multi-microchannel microfluidics in beagle dog models. *Int J Pharm.*, **608**: 121039.

Ling LB, Du YW, Ismail M, He RY, Hou YP, Fu ZL, Zhang Y, Yao C and Li XS (2017). Self-assembled liposomes of dual paclitaxel-phospholipid prodrug for anticancer therapy. *Int J Pharm.*, **526**(1-2): 11-22.

Liu J, Ye ZL, Xiang MX, Chang BC, Cui JY, Ji TT, Zhao L, Li QL, Deng Y, Xu LM, Wang GB and Wang L (2019). Functional extracellular vesicles engineered with lipid-grafted HA effectively reverse cancer drug resistance. *Biomaterials.*, **223**: 119475.

Ma, XD, Hu MQ, Wang H and Li JM (2018). Discovery of traditional Chinese medicine monomers and their synthetic intermediates, analogs or derivatives for battling P-gp-mediated multi-drug resistance. *Eur J Med Chem.*, **159**: 381-392.

Marinho A, Nunes C and Reis S (2021). Hyaluronic Acid: A key ingredient in the therapy of inflammation. *Biomolecules.*, **11**(10): 1518.

Nakamura T, Hiraoka K, Harada R, Matsuzawa T, Ishikawa Y, Funaki Y, Yoshikawa T, Tashiro M, Yanai K and Okamura N (2019). Brain histamine H_1 receptor occupancy after oral administration of desloratadine and loratadine. *Pharmacol Res Perspect.*, **7**(4): e00499.

Palumbo FS, Agnello S, Fiorica C, Pitarresi G, Puleio R, Loria GR and Giammona G (2017). Spray dried HA microparticles for adhesion controlled aggregation and potential stimulation of stem cells. *Int J Pharm.*, **519**(1-2): 332-342.

Sun W, Du Y, Liang XL, Yu CY, Fang JJ, Lu W, Guo XY, Tian J, Jin YH and Zheng JJ (2019). Synergistic triple-combination therapy with HA-shelled PPy/CPT nanoparticles results in tumor regression and prevents tumor recurrence and metastasis in 4T1 breast cancer. *Biomaterials.*, **217**: 119264.

Suzuki T (2020). Regulation of the intestinal barrier by nutrients: The role of tight junctions. *Anim Sci J.*, **91**(1): e13357.

Subramanian DA, Langer R and Traverso G (2022). Mucus interaction to improve gastrointestinal retention and pharmacokinetics of orally administered nano-drug delivery systems. *J Nanobiotechnology.*, **20**(1): 362.

Xia DN, He Y, Li QX, Hu CD, Huang W, Zhang YH, Wan F, Wang C and Gan Y (2018). Transport mechanism of lipid covered saquinavir pure drug nanoparticles in intestinal epithelium. *J Control Release.*, **69**: 159-170.

Yasen A, Herrera R, Rosbe K, Lien K and Tugizov SM (2018). HIV internalization into oral and genital epithelial cells by endocytosis and macropinocytosis leads to viral sequestration in the vesicles. *Virology.*, **515**: 92-107.

Zhang YT, Li Z, Zhang K, Zhang HY, He ZH, Xia, Zhao JH and Feng NP (2017). Co-delivery of evodiamine and rutaecarpine in a microemulsion-based HA hydrogel for enhanced analgesic effects on mouse pain models. *Int J Pharm.*, **528**(1-2): 100-106.